A Neural-Network Approach for Defect Recognition in TFT-LCD Photolithography Process

Li-Fei Chen, Chao-Ton Su, and Meng-Heng Chen

***Abstract*—Since the advent of high qualification and tiny technology, yield control in the photolithography process has played an important role in the manufacture of thin-film transistor-liquid crystal displays (TFT-LCDs). Through an auto optic inspection (AOI), defect points from the panels are collected, and the defect images are generated after the photolithography process. The defect images are usually identified by experienced engineers or operators. Evidently, human identification may produce potential misjudgments and cause time loss. This study therefore proposes a neural-network approach for defect recognition in the TFT-LCD photolithography process. There were four neural-network methods adopted for this purpose, namely, backpropagation, radial basis function, learning vector quantization 1, and learning vector quantization 2. A comparison of the performance of these four types of neural-networks was illustrated. The results showed that the proposed approach can effectively recognize the defect images in the photolithography process.**

***Index Terms*—Defect, liquid crystal display (LCD), neural-network, photolithography process, thin-film transistor (TFT).**

I. Introduction

THE thin-film transistor-liquid crystal display (TFT-LCD) market has grown rapidly in recent years and is expected to expand to grow twice its current size over the forecasted period. Because of the complicated manufacturing process and the expensive equipment, we can say that TFT-LCD manufacturing is a highly competitive industry. The photolithography process is a crucial step in the TFT-LCD manufacturing process. A low yield in this step may result in the loss of competitiveness; therefore, most of the TFT-LCD manufacturing firms take great efforts in improving their yield rates. Highly automated and precisely monitored facilities are used throughout the complex manufacturing process. Nonetheless, process variations still exist. Such process variations may arise from the manufacturing process itself, from equipment malfunctions, or from human mistakes and will undoubtedly affect the yield rate.

Manuscript received November 21, 2007; revised February 18, 2008. This work was supported by the National Science Council of Taiwan, R.O.C., under Contract NSC-96-2221-E-007-049. Current version published January 08, 2009. This work was recommended for publication by Associate Editor I. Fidan upon evaluation of the reviewers comments.

L.-F. Chen is with the Program of Global Entrepreneurial Management and Business Administration, College of Management, Fu Jen Catholic University, Hsinchuang, Taipei County 24205, Taiwan, R.O.C. (e-mail: d917809@alumni.nthu.edu.tw).

C.-T. Su and M.-H. Chen are with the Department of Industrial Engineering and Engineering Management, National Tsing Hua University, Hsinchu 30013, Taiwan, R.O.C.

Color versions of one or more of the figures in this paper are available online at http://ieeexplore.ieee.org.

Digital Object Identifier 10.1109/TEPM.2008.926117

Therefore, engineers attend to the investigation of these process variations in order to enhance the yield rate. Through an auto optic inspection (AOI), defects from the panels are collected and the defect images are generated after the photolithography process. Then, the defect images are identified by the experienced engineers or operators. However, this visual judgment method may lead to some inspection drawbacks such as human fatigue and time wastage.

Several existing methods have been proposed to address these identification defect problems [1]. Zhang *et al.* [2] developed an automatic post-sawing inspection system using computer vision techniques. This system used feature selection to recognize the defect images. Meanwhile, Chen and Liu [3] developed an intelligent system, which recognizes the defects in spatial patterns, to aid in the diagnosis of the causes of failure using the neural-network architectures ART1 and SOM. Finally, Su *et al.* [4] proposed a neural-network approach for semiconductor wafer post-sawing inspection. Such classification and recognition problems have been widely discussed and neural-network has shown its excellent performance in these problems. Chou *et al.* [5] described an automated defect classification system that classifies defects on semiconductor chips at various manufacturing steps.

Due to the neural-network's flexibility, robustness, high processing speed, and high identification rate [6], we proposed a neural-network approach for product defect recognition in the TFT-LCD photolithography process in this study. Four neural-network learning methods were proposed and tested, namely, backpropagation (BP), radial basis function (RBF), learning vector quantization 1 (LVQ1), and learning vector quantization 2 (LVQ2). The results showed that the proposed approach could indeed recognize the defect images more correctly and faster than the original method.

Section II of this study describes the product defect recognition problems in the TFT-LCD photolithography process. Section III details the discussions for the proposed approach. Finally, implementation results are discussed in Section IV and conclusions are given in Section V.

II. Defect Recognition Problem in TFT-LCD Photolithography Process

A. Photolithography Process

The TFT-LCD photolithography process is a crucial step because the panel quality depends on the entire pattern formation. The purpose of the process is to transfer a pattern from the photo mask onto a substrate. As shown in Fig. 1, there are three conceptual parts in the photolithography process: coating, exposure, and developing.

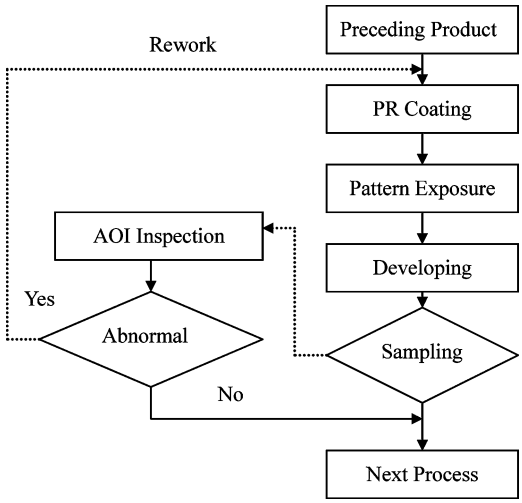

Fig. 1. Photolithography process flow.

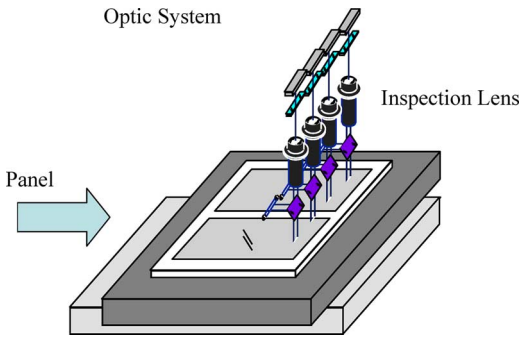

Fig. 2. AOI system.

The photolithography process begins when the substrate is coated with an extremely thin liquid film of photosensitive material. The light then exposes the photosensitive material, a part of which is destroyed when exposed to the light. The unnecessary portion of the material is then cleaned from the surface through another process, leaving an extremely fine pattern behind. Another layer of the photosensitive material is then deposited to the substrate, exposed, and cleaned until all the layers have been printed or imaged onto the surface.

After the photolithography process, an AOI is required before proceeding to the next process. The engineer will sample some panels and, if there are no defects found, the panel will undergo the next step. Otherwise, the panel will be reworked. The purpose of this inspection is to maintain quality and find out the causes of defects.

The AOI is precise and sensitive; its structure is shown in Fig. 2. Through the AOI, a defects list for each sampled panel is recorded. The engineers then check the defect images and find the causes of defects based on their own experiences.

B. Defect Recognition

Although the AOI records the defects list for each sampled panel, detailed reasons for the defects must be judged by the experienced engineers. The causes of defects may be attributed to many problems such as poor coating, scratch, and mist. The engineers must then find out for certain the specific defects. Because the AOI records the defects list for each sampled panel only, it apparently costs a lot of time and requires much effort from engineers to judge the defect problems. Fig. 3 illustrates the four commonly seen defect types in the photolithography process.

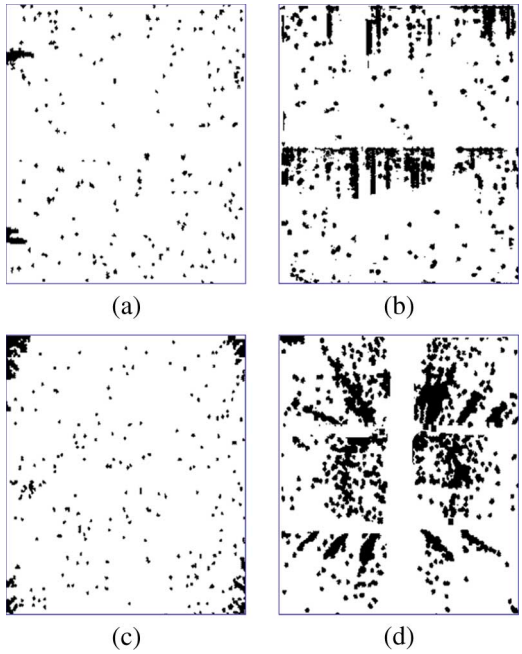

Fig. 3. Four commonly seen defect types in the photolithography process. (a) Etching machine scratch. (b) Laser anneal issue. (c) Poor coating. (d) Flatness layer globule issue.

TABLE I
DETAILED DEFECT TYPES UNDER THE THREE MAIN PROBLEM

Category	Defect Types
Manufacture Process Problem	White Point, Bubble, Color Abnormal Anneal, Metal Film Residue, Flatness Layer Peeling, Broken, Laser Anneal, Stripping Issue
Manufacture Machine Problem	Edge Remove Roller, Flatness Layer Globule Issue, Poor Coating, Stepper Ball Screw, Scratch, Poor Developing, Scratch, Mist
Inspection Machine Problem	Lens Sensitivity

From the past implementation results, there were about 17 defect types found in the photolithography process. These different kinds of defect types can be generalized into three main problem categories, namely, manufacture process problems, manufacture machine problems, and inspection machine problems. In a manufacture process problem, the existence of defects is caused by the inappropriate manufacture process setting. In a manufacture machine problem, the defects are caused by the manufacturing machine such as the malfunction or configuration issue of the machine. Finally, in an inspection machine problem, the settings of AOI are so sensitive that they cause abnormal inspection results. Grouping these 17 defect types into three main problem categories can help engineers detect the main problem more quickly and respond correctly. Table I shows the detailed defect types under the three main problem categories.

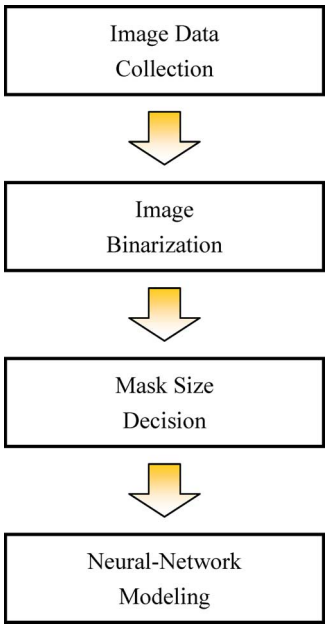

Fig. 4. Proposed approach.

III. Proposed Approach

We know too well the fecklessness of human judgment. Potential inspection errors may be introduced into the inspection process due to human fatigue. In addition, the time wastage may also be significant. Therefore, a systematic process is required to solve such problems. Neural-network has been proven to be an efficient tool in conducting classification problems in computer vision areas.

In this section, we proposed a neural-network-based inspection procedure. Fig. 4 details the process of this approach.

A. Image Data Collection

Valid input data are important in neural-network model learning. In an artificial intelligence approach, there are two critical points about data: number and representative. The sample defect images are collected uniformly in the three main problem categories (i.e., manufacture process, manufacture machine, and inspection machine problems). These defect images should include commonly seen defect types introduced in Table I and, of course, it may be better to collect as much image data as possible.

B. Image Binarization

The collected defect images look like the ones shown in Fig. 3. The original image has the true color. Because engineers judge the defect types only by their defect patterns, the pixel brightness does not affect the judgment at all. We can convert the brightness of each pixel to a binary level. The defect points are viewed as black points and the other points are viewed as white points. This action can be done oppositely. An example is shown in Fig. 5. Next, we can use software such as MATLAB to assign black points a value of 1 and assign white points a value of 0. Fig. 6 illustrates an example of the result.

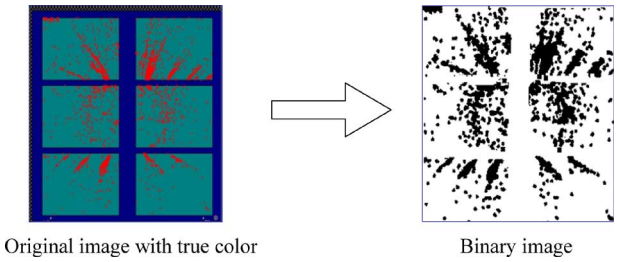

Fig. 5. Image conversion (defect points are viewed as black points) points.

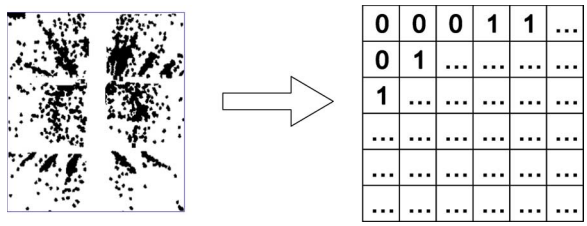

Fig. 6. Image binarization.

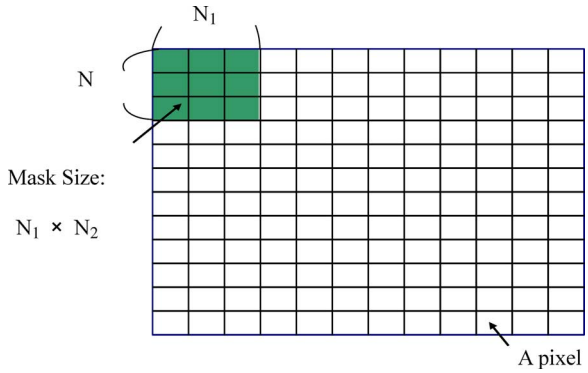

Fig. 7. Illustration of mask size.

C. Mask Size Decision

If we use each pixel to represent a neural-network input node, the number of neural-network inputs will then become intractable and will affect the efficiency of the neural-network model. Therefore, a proper mask size is defined to represent a neural-network input node. Mask size is defined as a rectangular area which is comprised of $N_1 \times N_2$ pixels. N_1 and N_2 are the number of pixels for rectangular length and width, respectively. Fig. 7 shows an example of an image comprised of 144 pixels (12×12) and a mask size comprised of nine pixels (3×3). Each mask represents an input node of neural-network model.

Next, we sum up the pixel values in the mask and divide it by the mask size to represent the input value of the neural-network input node. Fig. 8 illustrates a sample computation. Generally, the larger the mask is, the fewer the neural-network inputs will be. Fewer input nodes may affect the accuracy of the final result because there is no significance between the input nodes due to the large mask size. Similarly, larger input nodes may affect the efficiency of neural-network model because of the small mask size.

The determination of the input nodes is a tradeoff between model accuracy and model efficiency. In this paper, we use the concept of "cluster analysis" in order to decide the best mask

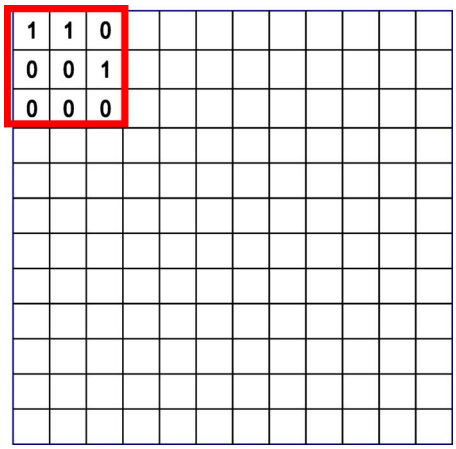

Fig. 8. Sample computation of neural-network input value.

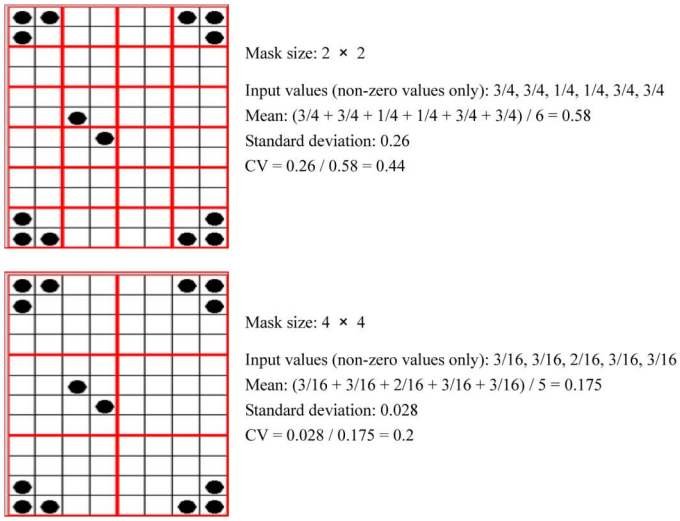

Fig. 9. Examples of determination of mask size.

size. The idea is that the masks (if they contain defects) can be seen as different clusters. The aim of clustering is to maximize the variation between different clusters and minimize the variation of the elements in the same cluster. We hope that the mask size can generate a larger variation in neural-network input values. Therefore, the index coefficient of variation (CV) is introduced to compare the variation between the different mask sizes. The CV for a binary image is defined as σ/μ, where σ and μ are the standard deviation and mean of nonzero values in the neural network input nodes, respectively. Please note that the collected image data usually contain many pixels. Too many zero input values will affect the selection of mask size; therefore, in this study, only nonzero values are taken into consideration. Fig. 9 shows the sample computations of the CV. We suggest selecting a proper mask size based on the criteria of "the larger the CV, the better the decision of the mask size will be."

D. Neural-Network Modeling

This part is the final step in the proposed approach. Four types of supervised neural-network are applied to the problem. As mentioned earlier, they are BP, RBF, LVQ1, and LVQ2. When these models are used, they require making an appropriate choice for the neural paradigm fine-tuning of the network topology in order to find a suitable structure between the performance and computational complexity.

The BP network usually has three or four layers: an input layer, an output layer, and one to two hidden layers. There are two user-defined parameters in a BP network which will affect the computation efficiency: learning rate and momentum. A general rule has been reported by Lippmann [7]. For more background reviews of the BP network, readers are referred to Fausett [8].

The RBF network has the same structure and parameters as the BP network; however, there is one hidden layer. Aside from this, there are no connection weights between the input layer and the hidden layer. Its learning process iteratively adjusts the center and shape of the receptive field function. The RBF network owns a simple structure and fast learning. Further information can be found in [9].

The LVQ network is a pattern classification method based on supervised training. There are two parameters in an LVQ: the number of Kohonen nodes for the output layer and the learning rate. This study utilized LVQ1 and LVQ2, the two most frequently used LVQ algorithms. In LVQ1, only the weight vector (for an output node) that is closest to the input vector is updated. Meanwhile, the idea of LVQ2's learning rule is that if the input is approximately the same distance from both the winner and the next-to-closest, then each of them should learn. Such a learning rule is especially suitable for data with overlap properties. Readers can find additional information on the LVQ network in [10].

We use testing samples to validate the developed model. Once a validated model is made available, it can be employed in an online implementation.

IV. Implementation

Actual data obtained from a TFT-LCD manufacturing company in Hsinchu, Taiwan, were used in the experiments. The image processing was performed by ACDSee 5.0 and MATLAB 7.0 on an Intel 1.6-G and 512-DRAM PC in a Windows XP environment. The neural-network training and testing was performed by Neural Works Professional II/PLUS v5.3.

A. Image Data Collection

In order to collect enough sample image patterns, we fully cooperated with the engineers to collect defect data. There were 20 defect data collected including ten manufacture process problem data, eight manufacture machine problem data, and two inspection machine problem data. Due to the difficulty in collecting sufficient defect data, we simulated various defect data to fit enough numbers for modeling. The detail allocations of sample data and simulated data are summarized in Table II.

This study simulated the defect data based on the original patterns. The defect types have their own main characteristics. By

TABLE II
ALLOCATIONS OF SAMPLE DATA AND SIMULATED

Patterns	Number of sample data	Number of simulated data	Total
Manufacture process	10	30	40
Manufacture machine	8	32	40
Inspection machine	2	38	40

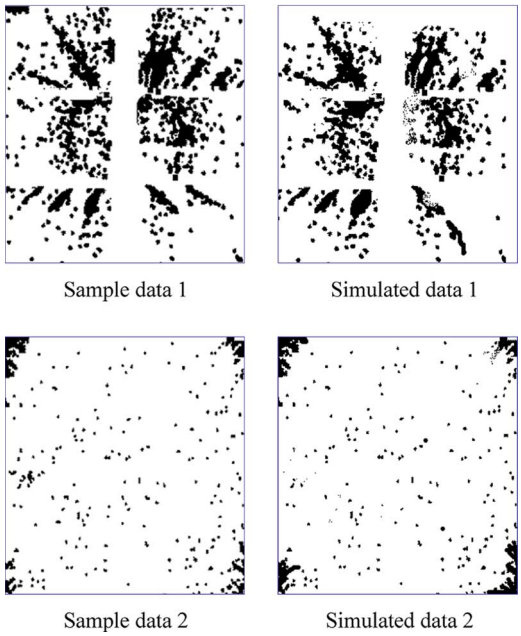

Fig. 10. Examples of simulated data.

these main characteristics, we simulated the other defect data. Fig. 10 shows the examples.

The purpose of simulated data is to ensure enough training patterns in neural-network modeling. The total number of defect data amounted to 120 including the sample and simulated data. The simulated data were all used as training patterns and the sample data were used as testing patterns. We can verify the model accuracy by the testing result since the testing patterns included real data. This allocation of training and testing can supplement the insufficient of real sample data.

B. Image Binarization

The defect images had true colors and contained about 500 $\times$ 450 pixels each. For a more convenient mask size decision, we used ACDSee 5.0 to adjust the collected defect images to 300 $\times$ 280 pixels images. This adjustment did not affect the inspection results because the main characteristics of the image patterns still existed. We also used ACDSee 5.0 to convert the brightness of each pixel to a binary level. After the defect images were converted to the binary, we used MATLAB 7.0 to change each pixel to a binary value.

TABLE III
MASK SIZES

Mask Size	Number of Input Nodes
30 x 28 (840)	100
25 x 28 (700)	120
25 x 20 (500)	168
20 x 20 (400)	210
15 x 20 (300)	280

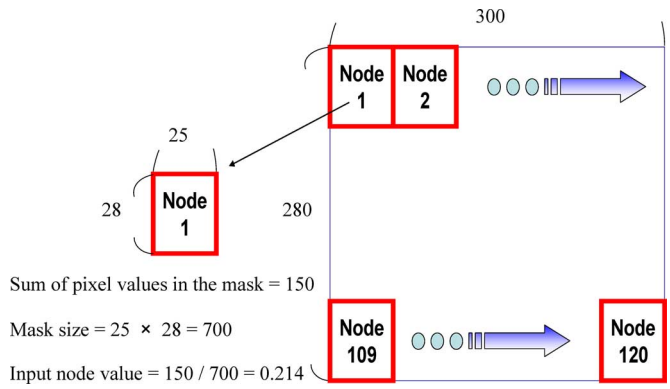

Fig. 11. Mapping address for an image with 120 masks.

TABLE IV
TRAINING AND TESTING GROUPS OF NEURAL-NETWORK DATA

Category	Number of Manufacture Process Data	Number of Manufacture Machine Data	Number of Inspection Machine Data
Training group	30	30	30
Testing group	10	10	10

C. Mask Size Decision

In order to determine the corresponding neural-network input nodes, this study used five different mask sizes as shown in Table III. The number of input nodes was the quotient of image size $(300 \times 280 = 84\,000)$ and its mask size. For instance, when the mask size is $(25 \times 28 = 700)$ pixels, then the number of input nodes is $(300 \times 280)/(25 \times 28) = 120$. Generally, the larger the mask, the fewer the neural-network inputs. The results are shown in Table III.

After the mask size is defined, the sum of binary values in the mask divided by the mask size is used to represent one neural-network input node. For example, when the mask size is $(25 \times 28 = 700)$ pixels and the sum of binary values in one mask is 150, then the mapping neural-network input is $150/700 = 0.214$. The resulting mapping address (input node number) and the sample neural-network input are illustrated in Fig. 11.

TABLE V
NEURAL-NETWORK PARAMETERS SETUPS

	Mask Size	No. of Input Nodes	Learning Iterations	Learning Rate	Momentum
BP	30 × 28	100	90000	0.7	0.3
	25 × 28	120	90000	0.7	0.3
	25 × 20	168	90000	0.7	0.3
	20 × 20	210	90000	0.7	0.3
	15 × 20	280	90000	0.7	0.3
RBF	30 × 28	100	90000	0.7	0.3
	25 × 28	120	90000	0.7	0.3
	25 × 20	168	90000	0.7	0.3
	20 × 20	210	90000	0.7	0.3
	15 × 20	280	90000	0.7	0.3
LVQ1	30 × 28	100	54000	0.06	N / A
	25 × 28	120	54000	0.06	N / A
	25 × 20	168	54000	0.06	N / A
	20 × 20	210	54000	0.06	N / A
	15 × 20	280	54000	0.06	N / A
LVQ2	30 × 28	100	54000	0.03	N / A
	25 × 28	120	54000	0.03	N / A
	25 × 20	168	54000	0.03	N / A
	20 × 20	210	54000	0.03	N / A
	15 × 20	280	54000	0.03	N / A

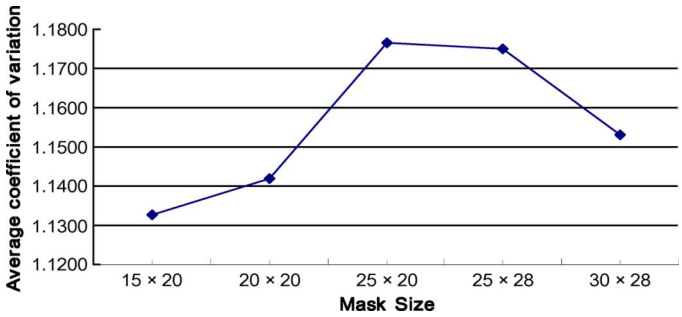

Fig. 12. Average CV comparison decisions result.

Next, by using 120 samples, we compute the average CV for each mask size. Fig. 12 shows the results; the mask size with 15 × 20 pixels should be our best choice.

D. Neural-Network Modeling

The 120 samples were separated into two groups, training and testing, as shown in Table IV. There were 90 training data and 30 testing data for neural-network modeling. The training data were all simulated data, whereas most of the testing data included real data. Next, we set the parameters for neural-network model training. Learning iteration, learning rate, momentum, and the number of nodes in the hidden layer are usually the four parameters for neural-network model training. LVQ1 and LVQ2 have no momentum parameters. The root-mean-square error (RMSE) is used for measuring the neural-network modeling errors and is defined as

$$\text{RMSE} = \frac{1}{n}\sqrt{\sum_{i=1}^{n}(y_i - \widehat{y}_i)^2} \tag{1}$$

where n, y_i, and $\widehat{y}_i$ are the number of samples, actual response of sample, and predicted response of sample, respectively. We first fixed the momentum and the learning rate at a predetermined level. Then, the model training continued until a stable and acceptable RMSE was obtained. Experimental results showed that the decision of iteration number is not sensitive to momentum and learning rate. Therefore, some commonly seen values were set; for example, 0.1, 0.2, ..., 0.9 are set for different learning rates and momentum levels. Through several trial-and-error iterations, the learning rate, momentum, and number of hidden nodes were chosen. The results are summarized in Table V.

For each step in Table V, we trained a neural-network using a different number of nodes in the hidden layer (or Kohonen layer in LVQ1, LVQ2). We then chose the best one based on the following criteria: 1) the higher the accuracy, the better the neural-network model; 2) minimal RMSE from the training data; 3) minimal RMSE from the testing data; 4) minimal discrepancy between RMSEs from training and testing data. Table VI summarizes the best number of nodes for each step and indicates the best setup for each type of neural-network.

TABLE VI
NEURAL-NETWORK MODELING

	Mask Size	No. of Input Nodes	Best No. of Nodes in Hidden Layer	Accuracy
BP	30 × 28	100	22	77%
	25 × 28	120	32	90%
	25 × 20*	168	12	93%
	20 × 20	210	12	80%
	15 × 20	280	18	77%
RBF	30 × 28	100	32	80%
	25 × 28	120	26	83%
	25 × 20*	168	32	87%
	20 × 20	210	40	80%
	15 × 20	280	36	73%
LVQ1	30 × 28	100	30	80%
	25 × 28	120	21	80%
	25 × 20*	168	33	93%
	20 × 20	210	30	87%
	15 × 20	280	9	80%
LVQ2	30 × 28	100	33	90%
	25 × 28	120	30	93%
	25 × 20*	168	33	97%
	20 × 20	210	12	90%
	15 × 20	280	18	83%

∗ Best setup

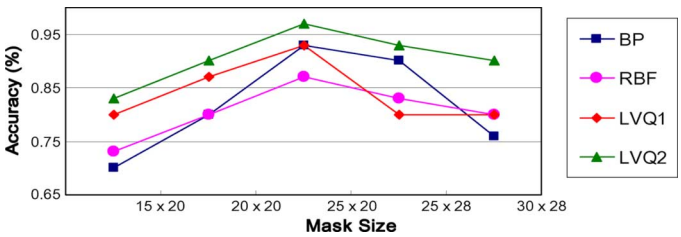

Fig. 13. Accuracy comparisons for four types of networks.

The accuracy is represented by the number of correctly classified examples. Fig. 13 compares the differences in performance for the four types of networks according to Table VI.

The best setup in terms of accuracy was found to have a mask size of 500 (25 × 20) for all four types of neural-networks. In addition, the mask size of 300 (15 × 20) was found to be inferior to the other four mask sizes. These results confirmed that our proposed mask size decision method can effectively provide defect identification in terms of accuracy. Moreover, as shown in Fig. 13, LVQ2 had better inspection results than the other three networks while RBF showed inferior results.

E. Comparison

The processing time for the proposed approach to recognize one defect image in this case study is less than 0.5 s and the visual judgment, for a highly experienced inspector, takes about 3 s. The difference is quite significant. Although the training of neural-network involves some procedures, it is conducted only once. The time assumed for training an employee to become a highly experienced inspector is more than one month. In the case of the company, an average of 400 defect images is judged each day. This means a company spends at least 1200 (3 × 400) s on this procedure per day, and yet, only 200 s per day are needed when the proposed approach is used. Thus, it is an amazing progress in capacity, not to mention a vast amount in savings.

The proposed approach uses neural-network in recognizing defect patterns. There are still two commonly used methodologies for defect recognition, that is, visual and digital image processing. The accuracy of visual judgment depends a lot on human faculties. To improve the process, digital image processing was developed. Digital image processing uses computer vision and focuses on the feature extraction of defect patterns. It is usually concluded in five steps: image acquisition, image enhancement, image restoration, image segmentation, and image recognition.

Compared to digital image processing, the proposed approach is easier for model building because the model training process is simpler and the required domain knowledge is lesser. We find that the proposed approach is superior to the use of visual judgment in many factors such as speed, accuracy, and cost. However, the proposed approach is inferior in terms of system setup lead-time and flexibility to product complexity. Visual judgment may perform well in a high-variety and low-volume

manufacturing system. Meanwhile, when the partial panel area is adequate to present the defect type, the digital image processing method may be the best methodology. In a low-variety and high-volume manufacturing system; however, the proposed approach is the most efficient and effective method.

V. Conclusion

Photolithography process inspection plays an important role in TFT-LCD manufacturing. Traditionally, the defect images are identified by experienced engineers or operators. However, potential inspection errors may be introduced into the inspection process due to human fatigue. In addition, this visual judgment method also requires significant operation time. To solve this problem, we proposed in this study a neural-network approach for inspecting the photolithography process. We used the index coefficient of variation to decide the best mask size; thereby, the neural network input node value can be determined. Four types of neural-network were proposed, namely, BP, RBF, LVQ1, and LVQ2. The findings showed that LVQ2 had better inspection results than the other three networks while RBF had inferior results. In terms of accuracy, the implementation results also showed promise for the proposed approach in solving real-world applications. Moreover, we used the coefficient of variation to find out the best mask size. The results also showed promise for the proposed approach.

With some modifications in the neural-network models employed in this study, a higher inspection accuracy may be obtained for the photolithography process. This may also be one of the directions of future research.

Acknowledgment

The authors would like to thank Process Manager Mr. C.-I. Huang for his full support and the use of the data in this study.

References

[1] C. Weber, B. Moslehi, and M. Dutta, "An integrated framework for yield management and defect/fault reduction," *IEEE Trans. Semicond. Manuf.*, vol. 8, no. 2, pp. 110–120, May 1995.

[2] J.-M. Zhang, R.-M. Lin, and M.-J. J. Wang, "The development of an automatic post-sawing inspection system using computer vision techniques," *Comput. Ind.*, vol. 40, pp. 51–60, 1999.

[3] F.-L. Chen and S.-F. Liu, "A neural-network approach to recognize defect spatial pattern in semiconductor fabrication," *IEEE Trans. Semicond. Manuf.*, vol. 13, no. 3, pp. 366–373, Aug. 2000.

[4] C.-T. Su, T. Yang, and C.-M. Ke, "A neural-network approach for semiconductor wafer post-sawing inspection," *IEEE Trans. Semicond. Manuf.*, vol. 15, no. 2, pp. 260–266, May 2002.

[5] P. B. Chou, A. R. Rao, M. C. Sturzenbecker, F. Y. Wu, and V. H. Brecher, "Automatic defect classification for semiconductor manufacturing," *Mach. Vision Applicat.*, vol. 9, no. 4, pp. 210–214, 1997.

[6] D. Barschdorff and L. Monostori, "Neural networks: Their applications and perspectives in intelligent machining," *Comput. Ind.*, vol. 17, pp. 101–119, 1991.

[7] R. P. Lippmann, "An introduction to computing with neural nets," *IEEE Acoust., Speech, Signal Process. Mag.*, vol. 4, no. 2, pp. 4–22, Apr. 1987.

[8] L. Fausett, *Fundamentals of Neural Networks*. Englewood Cliffs, NJ: Prentice-Hall, 1994.

[9] J.-S. R. Jang, C.-T. Sun, and E. Mizutani, *Neuro-Fuzzy and Soft Computing*. Upper Saddle River, NJ: Prentice-Hall, 1997.

[10] V. K. Gupta, J. G. Chen, and M. B. Murtaza, "A learning vector quantization neural network model for the classification of industrial construction projects," *Omega*, vol. 25, no. 6, pp. 715–727, 1997.

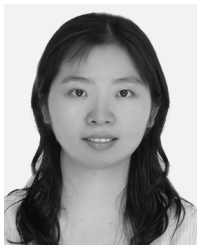

Li-Fei Chen received the Ph.D. degree in industrial engineering and engineering management from the National Tsing Hua University, Hsinchu, Taiwan, R.O.C.

She is an Assistant Professor in the Program of Global Entrepreneurial Management and Business Administration, College of Management, Fu Jen Catholic University, Taipei, Taiwan. Her research works appear in IEEE Transactions on Semiconductor Manufacturing, *Expert Systems with Applications*, and *Journal of Quality*. Her research interests include data mining, quality engineering, total quality management, and human resource management.

Chao-Ton Su received the Ph.D. degree in industrial engineering from the University of Missouri, Columbia.

He is a Chair Professor in the Department of Industrial Engineering and Engineering Management, National Tsing Hua University, Hsinchu, Taiwan, R.O.C. From 1985 to 2004, he was a Faculty Member in the Department of Industrial Engineering and Management, National Chiao Tung University, Hsinchu. Since August 2006, he has been a Tsing Hua Distinguished Professor. His research activities include quality engineering and management, operation management, and neural networks in industrial applications.

Prof. Su is a member of the Institute of Industrial Engineers (IIE), Chinese Institute of Industrial Engineers (CIIE), and Chinese Society for Quality (CSQ) and a senior member of the American Society for Quality (ASQ). He is a two-time recipient (2000–2001 and 2002–2005) of the Outstanding Research Award from the National Science Council, Taiwan. In 2001, he also received the Individual Award of the National Quality Awards of the Republic of China.

Meng-Heng Chen received the M.S. degree in industrial engineering and engineering management from the National Tsing Hua University, Hsinchu, Taiwan, R.O.C., in 2007.

He is currently in the army. His research interests include data mining and quality engineering.